



CHORUS

This is the accepted manuscript made available via CHORUS. The article has been published as:

Monte Carlo study of a $U(1) \times U(1)$ system with π -statistical interaction

Scott D. Geraedts and Olexei I. Motrunich

Phys. Rev. B **85**, 045114 — Published 17 January 2012

DOI: [10.1103/PhysRevB.85.045114](https://doi.org/10.1103/PhysRevB.85.045114)

Monte Carlo study of a $U(1) \times U(1)$ system with π -statistical interaction

Scott D. Geraedts and Olexei I. Motrunich

Department of Physics, California Institute of Technology, Pasadena, California 91125, USA

(Dated: January 3, 2012)

We study a $U(1) \times U(1)$ system with two species of loops with mutual π -statistics in (2+1) dimensions. We are able to reformulate the model in a way that can be studied by Monte Carlo and we determine the phase diagram. In addition to a phase with no loops, we find two phases with only one species of loop proliferated. The model has a self-dual line, a segment of which separates these two phases. Everywhere on the segment, we find the transition to be first-order, signifying that the two loop systems behave as immiscible fluids when they are both trying to condense. Moving further along the self-dual line, we find a phase where both loops proliferate, but they are only of even strength, and therefore avoid the statistical interactions. We study another model which does not have this phase, and also find first-order behavior on the self-dual segment.

I. INTRODUCTION

Systems with statistical interactions between particles arise in many contexts. For example, Laughlin quasi-particles in the fractional Quantum Hall Effect have mutual statistics which depends on the particular state.¹ As another example, spinon and vison excitations in Z_2 fractionalized phases in quantum magnets have mutual π statistics.²⁻⁴

While gapped topological phases are well understood, the phase transitions between them are less explored. One reason is that the character of the transitions is a dynamical question, while in cases with statistical interactions, the system path integral contains generally complex phases and hence has sign problem in direct Monte Carlo (MC) approaches.

References 5 and 6 considered the toric code model, which can be also viewed as an Ising gauge theory with Ising matter fields.⁷ In a formulation containing Ising matter and Z_2 fluxes (visons) as elementary particles, the two have π -statistical interaction, and one cannot simulate large systems in these degrees of freedom. On the other hand, the matter-gauge field formulation does not have the sign problem and was studied in detail in MC.⁶ This system has two phases:⁷ deconfined and confined. The confined phase includes both the Higgs regime (crudely viewed as condensation of matter out of the deconfined phase) and confining regime (viewed as condensation of visons), and there is a path connecting the two regimes that does not cross any phase transitions. Resembling somewhat liquid-gas system, there is also a finite segment of first-order transitions separating the two regimes along the so-called self-dual line, where the Z_2 charges and Z_2 vortices have identical interactions. We can think of the two species as being immiscible on the first-order segment. Reference 6 focused on the transition near the tip of the deconfined phase along the self-dual line and possible scenarios how the Higgs and confinement transition lines join.

In this paper, we study a $U(1) \times U(1)$ system with π statistical interactions, which appears in effective field theories of frustrated quantum antiferromagnets⁸⁻¹⁰ and other areas.^{11,12} We consider concrete lattice realizations that can be reformulated in a sign-free manner and explore these using MC.

Specifically, we consider a system of two loops with short-

range interactions and $\theta = \pi$ statistics,

$$S = \sum_r \frac{\vec{J}_1(r)^2}{2t_1} + \sum_R \frac{\vec{J}_2(R)^2}{2t_2} + i\theta \sum_r \vec{J}_1(r) \cdot \vec{a}_2(r). \quad (1)$$

The index r refers to sites on a cubic lattice (the “direct” lattice), and R refers to sites on another, inter-penetrating cubic lattice (the “dual” lattice)¹³. $J_{1\mu}(r)$ is an integer-valued current on a link $r, r + \hat{\mu}$ of the direct cubic lattice, $J_{2\mu}(R)$ is integer-valued current on a link $R, R + \hat{\mu}$ of the dual cubic lattice. We use schematic vector notation so that \vec{J}_1 and \vec{J}_2 represent these conserved integer-valued currents, and $\vec{\nabla} \cdot \vec{J}_1 = 0, \vec{\nabla} \cdot \vec{J}_2 = 0$. In the partition sum, a given current configuration obtains a phase $e^{i\pi}$ for each cross-linking of the two loop systems. This is realized in the last term of Eq. (1), by including an auxiliary “gauge field” \vec{a}_2 , defined on the direct lattice, whose flux encodes the \vec{J}_2 currents, $\vec{J}_2 = \vec{\nabla} \times \vec{a}_2$. Just like in the $Z_2 \times Z_2$ case, we can reformulate the model as a special matter-gauge system amenable to MC study.

Figure 1 is our main result and shows the phase diagram of this model. For small t_1 and t_2 , there are only small loops (phase 0 in the figure). If we fix t_2 and increase t_1 , the J_2 loops remain small, while beyond some critical t_1 coupling, J_1 loops condense via an XY transition (phase I); we get another phase (II) if we keep t_1 small and increase t_2 . For $t_1 = t_2$, the model is symmetric under $J_1 \leftrightarrow J_2$, and so the model is self-dual on this line, similarly to the self-dual line in the Ising matter plus Ising gauge theory viewed as two species of Ising particles with π -statistics mentioned earlier. Unlike the Ising case, the two phases I and II are distinct, and the following question arises. Suppose we are increasing t_1 and t_2 along the self-dual line $t_1 = t_2 = t$ where the two species have identical interactions, so both equally want to proliferate at some point. One possibility is that they behave as immiscible fluids and phase separate. Another possibility is a regime where both loops are present in some critical soup, which would be an example of an unusual phase transition. Such a question is of much recent interest.^{8,14-32}

In the present study we find that in the above specific model, the first scenario happens and we have first-order transition between phases I and II. Interestingly, if we continue increasing t_1 and t_2 , the two loops eventually condense simultaneously but only in even strength for both J_1 and J_2 , while there are no large loops of odd strength for either species. By go-

ing into this “paired- J_1 ” and “paired- J_2 ” phase (labelled III in Fig. 1), the loops avoid the destructive interference effects of the statistical interaction – intuitively, because the second term of Eq. (1) provides a contribution to the partition function of $\exp[i\pi \times (\text{even number})] = 1$.

Returning to the transition line I-II, the first-order transition is strongest near the two ends of the segment where respectively phase 0 or III opens up. We also explore what happens when we modify the model to eliminate phase III, which we realize by simply restricting $|J_1| \leq 1, |J_2| \leq 1$, thus preventing pairing within each species. The strength of the first-order character indeed decreases as we increase t , but for all such accessible values the transition remains first order.

II. MODEL AND MONTE CARLO METHOD

In order to reformulate Eq. (1) in a sign-free way, we pass from J_1 variables to conjugate 2π -periodic phase variables by formally writing the constraint at each r :

$$\delta[\vec{\nabla} \cdot \vec{J}_1(r) = 0] = \int_{-\pi}^{\pi} d\phi_r \exp[-i\phi_r(\vec{\nabla} \cdot \vec{J}_1)]. \quad (2)$$

To be precise in our system with periodic boundary conditions, we also require total currents of J_1 and J_2 to vanish. In this case we can write $\vec{J}_2 = \vec{\nabla} \times \vec{a}_2$ and the action (1) is independent of the gauge choice for a_2 . We enforce the zero current in J_1 with the help of fluctuating boundary conditions for the ϕ -s across a single cut for each direction $\mu = x, y, z$

$$\delta\left(\sum_r J_{1\mu}(r)\delta_{r,\mu,0}\right) = \int_{-\pi}^{\pi} d\gamma_\mu \exp[-i\gamma_\mu \sum_r J_{1\mu}(r)\delta_{r,\mu,0}]. \quad (3)$$

This gives the following partition function:

$$Z = \sum_{\text{constrained } \vec{J}_2} \int_{-\pi}^{\pi} \prod_r d\phi_r \int_{-\pi}^{\pi} \prod_{\mu=1}^3 d\gamma_\mu e^{-S[\phi, \gamma, a_2]} \quad (4)$$

where the action is given by:

$$S[\phi, \gamma, a_2] = \sum_r \frac{[\vec{\nabla} \times \vec{a}_2(r)]^2}{2t_2} + \sum_{r,\mu} V_{\text{Villain}}[\phi_{r+\mu} - \phi_r - \theta a_{2\mu}(r) - \gamma_\mu \delta_{r,\mu,0}] \quad (5)$$

V_{Villain} is the ‘Villain potential’, which is obtained by summing over the J_1 variables:

$$\exp[-V_{\text{Villain}}(\alpha, t_1)] = \sum_{J_1=-\infty}^{\infty} \exp\left[-\frac{J_1^2}{2t_1} + iJ_1\alpha\right] \quad (6)$$

In the actual Monte Carlo, we use $\phi_r, \gamma_\mu \in (-\pi, \pi)$, $a_{2\mu}(r) \in \mathbb{Z}$, and perform unrestricted Metropolis updates. One can show that physical properties measured in such a simulation are precisely as in the above finitely defined model.

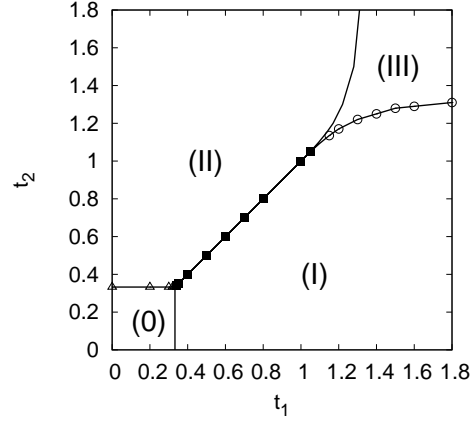


FIG. 1. The phase diagram for the unrestricted model. Phase (0) contains no loops. Phase (I) contains proliferated loops in J_1 and no loops in J_2 , while in phase (II) the variables are interchanged. Phase (III) contains proliferated double-strength loops in both variables.

In this work, we monitor “internal energy per site”, $\epsilon = S/L^3$, and compute heat capacity, defined as

$$C = (\langle \epsilon^2 \rangle - \langle \epsilon \rangle^2) \times \text{Vol}, \quad (7)$$

where $\text{Vol}=L^3$ is the volume of the system. To determine the phase diagram, we monitor loop behavior by studying “superfluid stiffness”, which is defined for loops of flavor a as:

$$\rho_a^{\mu\mu}(q) = \frac{1}{\text{Vol}} \left\langle \left| \sum_r J_{a\mu}(r) e^{i\vec{q}\cdot\vec{r}} \right|^2 \right\rangle. \quad (8)$$

Because of the vanishing total current, we define these at the smallest non-zero q ; e.g., for ρ^{xx} we used $\vec{q} = (0, \frac{2\pi}{L}, 0)$ and $\vec{q} = (0, 0, \frac{2\pi}{L})$. We focus on flavor 2 since it is more readily accessible in the formulation of (5). We also monitor gauge-invariant “magnetization”, defined as: $M = \sum_r e^{2i\phi_r}$, which can detect flavor 1 condensates (care is needed interpreting M for different boundary conditions).

III. RESULTS FOR UNRESTRICTED CURRENTS

We determined the phases of this model by looking at the order parameters ρ_2 and M . ρ_2 is non-zero in phases (II) and (III), and M is non-zero in phases (I) and (III). We found the locations of the phase boundaries more accurately by studying $\rho_2 \cdot L$ crossings. We took data in sweeps across the phase diagram (see Fig. 1), and defined the intersection of the $\rho_2 \cdot L$ curves to be the location of the phase transition. An example of such a sweep is shown in Fig. 3. The sweep is ‘vertical’ in the phase diagram, i.e. fixed t_1 . The symbols on the phase diagram are the values of t_1 at which the sweeps were performed. We studied the fine nature of the phases by looking at clusters formed by J_2 loops. In phase (II), the largest clusters of J_2 grow with system size, and have arbitrary J_2 , so we deduced that this phase contains condensed loops of J_2 . In phase (III), the loops that scale with system size have even J_2 ,

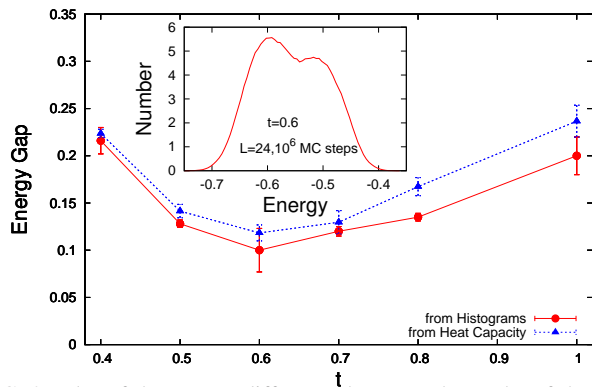


FIG. 2. Plot of the energy difference between the peaks of the histograms, as a function of $t_1 = t_2 = t$ on the self-dual line. Higher values denote a stronger first-order nature. The inset shows the energy histogram for $t_1 = t_2 = 0.6$. The dual-peaked shape of the histogram implies a first-order transition. The histograms were performed at $L = 24$ with 10^6 Monte Carlo sweeps. The heat capacity intercepts were found using data from $L = 8, 10, 12, 14$ and 16 .

so we judged that the condensed loops have even strength. In phases (0) and (I), we found no large clusters, and deduced that J_2 is gapped. The model with $t_1 = 0$ is a model containing only one species of loop³³. Our value for the position of the (0)-(II) XY transition ($t_2 \approx 0.333\dots$) is in agreement with prior work on this model³⁴. For $t_1 \rightarrow \infty$, the Villain weight (6) vanishes except for $\alpha = 2\pi \times (\text{int})$, which enforces $J_2 = \vec{\nabla} \times \vec{a}_2 = 2 \times (\text{int})$. Therefore, at large t_1 the (I)-(III) transition is a transition from no loops of J_2 to loops of even J_2 . One expects that this transition is XY-like, and similar to the (0)-(II) transition, but due to doubled J_2 , it should occur at a t_2 value four times higher. We observed the (I)-(III) transition to occur at $t_2 \approx 1.3$ for large t_1 , in agreement with this expectation.

To determine whether the loops are immiscible, or if a critical state is possible, we consider whether the phase transition (I)-(II) on the self-dual line is first- or second-order. We studied this by looking at histograms of ϵ . In the continuous case, these histograms would be singly-peaked, while in the first-order case we expect to see two distinct peaks. An example of such a histogram is shown in the inset for Fig. 2. We observed dual-peaked histograms for all points on the self-dual line. Therefore, we concluded that the transition is first-order. One way to quantify the strength of the transition is to look at the distance between the two peaks in these histograms. We plotted this peak-to-peak distance in Fig. 2, which is clearly non-zero for all t . Though this estimate of peak-to-peak distance comes from $L = 24$, we have produced similar histograms for different sizes and found no noticeable dependence of the peak-to-peak distance on system size.

We can also determine the order of the transition by looking at the heat capacity, where the signature of first-order is C growing as L^3 . Phenomenologically³⁵, at a first-order transition the energy distribution is described by a sum of two normal distributions, $P(\epsilon) = c_+ p_+ + c_- p_-$, where c_+ and c_- are the weights representing how much time the system

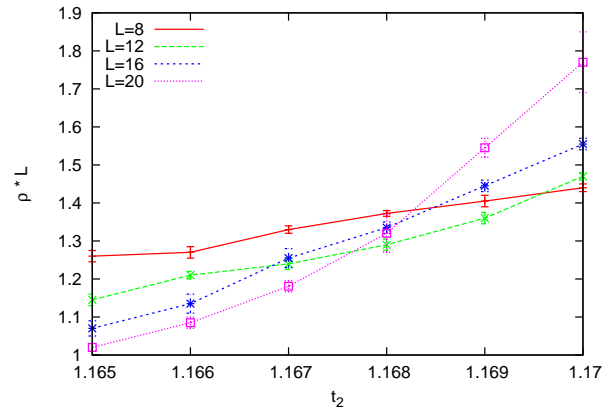


FIG. 3. $\rho_2(q_{min}) \cdot L$ as a function of t_2 at $t_1 = 1.2$. Based on this data, we conclude that the phase transition occurs at approximately $t_2 = 1.168$, and is second order in nature. Scans like this were used to determine the phase diagram in Fig. 1. Here the transition is between (I) and (III). Each data point is the result of 5×10^6 Monte Carlo sweeps. Error bars were determined by looking at the difference between runs with different initial conditions.

spends in each state, and p_+ and p_- are two normal distributions centered at ϵ_+ and ϵ_- . Computing heat capacity based on this ansatz gives:

$$\frac{C}{\text{Vol}} = c_+ c_- (\epsilon_+ - \epsilon_-)^2 + \frac{B}{\text{Vol}} = A + \frac{B}{\text{Vol}}, \quad (9)$$

where $\epsilon_+ - \epsilon_-$ is the peak-to-peak distance, and B is a volume-independent constant. We plotted $\frac{C}{\text{Vol}}$ vs. $\frac{1}{\text{Vol}}$ and found the y-intercepts of these plots, which should be equal to A . If we assume that $c_+ = c_- = 0.5$ as a rough estimate, then the energy gap should be equal to $2\sqrt{A}$. The resulting estimate from heat capacity is plotted in Fig. 2. It agrees well with our estimates from gaps in the energy histograms, which gives us confidence when we apply this phenomenological method to the restricted model. Both of our measurements of the energy gap show that the transition is strongly first-order at $t = 0.4$. The strength of the transition initially decreases with increasing t , before increasing again after $t \approx 0.6$. Thus, in this model the two condensates are immiscible.

In addition to finding the position of the phase boundaries, plots of $\rho_2 \cdot L$ like the one in Fig. 3 can be used to study the nature of the (I)-(III) phase transition. We can argue that at high t_1 , the phase transition is continuous. We are interested in whether the nature of the transition changes to first order before it meets up with the transition on the self-dual line. In a first-order transition, we expect the values of the $\rho_2 \cdot L$ crossings to increase with L . We do not observe this in Fig. 3, or plots at other t_1 . We therefore suspect that the transition is second-order, though our data is not precise enough to rule out a weak first-order transition. We also obtained histograms of the energy and magnetization at the phase transition located by the $\rho_2 \cdot L$ plots. We found no evidence of two peaks at $L = 16, 20$. Since we do not know the critical point exactly, it is difficult to study such histograms at larger sizes, so once again the data indicates a second-order transition but cannot rule out a weak first-order one.

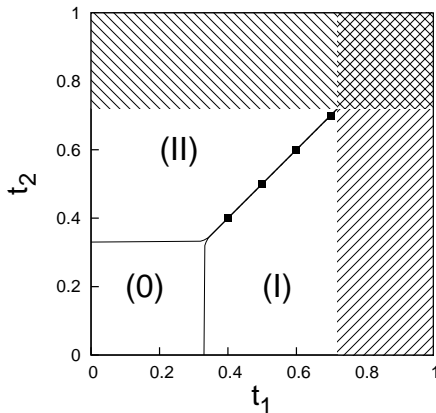


FIG. 4. The phase diagram of the ‘restricted’ model. The region with $+45^\circ$ lines is inaccessible in the formulation (5), and the cross-hatched region is inaccessible in this work. The transition is first order everywhere on the accessible portion on the self-dual line, but the strength decreases as t is increased.

IV. RESULTS FOR THE MODEL WITH RESTRICTED CURRENTS

From Fig. 2, we have seen that the first-order character of the phase transition on the self-dual line is strongest where it meets phases (0) and (III). Therefore we might expect the transition to be more weakly first-order if we could eliminate phase (III). This is the reasoning behind the restricted model, where we only allow loops with $|J_1| \leq 1$, $|J_2| \leq 1$. This has been done in the Monte Carlo by only changing a_2 if the resulting curl satisfies the restrictions, and by restricting the sum in Eq. (6) to run only over the values $-1, 0, 1$.

Figure 4 shows the phase diagram for this modified system, which was determined using the same methods as Fig. 1. The boundaries of phase (0) are very similar to the unrestricted model, which is not surprising as at the (0)-(I) transition the proliferating loops are mostly of strength 1. Referring to the Villain potential (6), we see that if the sum on the right side is negative, the potential is undefined. When the sum is restricted to $|J_1| \leq 1$, this occurs for $t_1 \gtrsim 0.72135$, and this limits the area of the phase diagram that we can study with this formulation. Upon using interchange symmetry, Fig. 4 contains a region inaccessible in this work, indicated by cross-hatching.

We now investigate whether removing phase (III) has changed the nature of the transition on the self-dual line. We used energy histograms and studies of the heat capacity to determine the peak-to-peak distance. The heat capacity suggests a first-order transition, as shown in Fig. 5. For completeness, we have also shown the original data which this figure is based on, in Fig. 6. For $t = 0.6, 0.7$, the energy gaps were too small to be accurately determined by studying the histograms. The histogram for $t = 0.7$ is shown in the inset to Fig. 5. We cannot resolve two separate peaks, but the distribution has a flat top, which suggests that the transition is weakly first-order. In order to acquire more clearly two-peaked histograms, we studied the magnetization of the system. We found the peaks in these to be more easily distinguished, and the results clearly

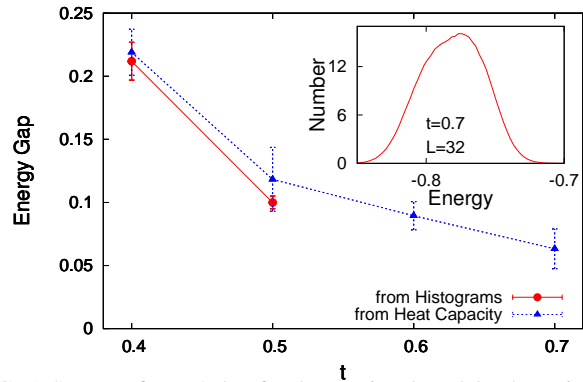


FIG. 5. Same as figure 2, but for the restricted model. The estimates from the heat capacity come from the y-intercepts in Fig. 6.

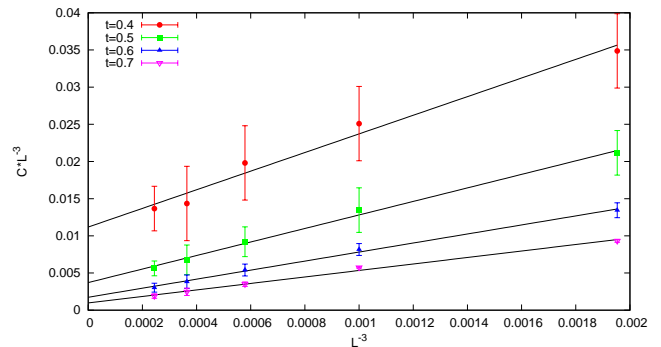


FIG. 6. C/L^3 vs. $1/L^3$ for the restricted model. The data shows non-zero y-intercepts for all t , confirming the first-order nature of the transition on the self-dual line. The black lines are least-squares fits to the data, and uncertainties come from comparing runs with different initial conditions

indicate a first-order transition.

V. DISCUSSION

We studied a lattice realization of a $U(1) \times U(1)$ system with π -statistical interactions. It was helpful to know the location of the phase transition between I and II from self-duality in this non-trivial 3D Statistical Mechanics problem. In two somewhat different models, we found first-order transitions on the self-dual line, which means that when both loops are trying to condense, they tend to phase-separate. A continuous transition would be an example of an NCCP¹ $U(1)$ self-dual critical point⁸. We found in the restricted model that the first-order transition became weaker as t was increased, but we could not study the model for t higher than a certain value. If one could find a way to study the model at high t , it would be interesting to see if the first-order transition continues to weaken and perhaps becomes second-order. One could also explore more models asking if some short-range modifications can produce a critical loop state. There is evidence for a continuous transition in $SU(2)$ spin models,^{16,17,26,27} but our system has no analog to these.

Our study is an example of a sign-free reformulation of a model with statistical interactions and the power hence afforded by Monte Carlo to establish the phase diagrams and study phase transitions.^{6,36} Though we determined most of the phase diagram in good detail, it may be useful to get a better understanding of how the phase transitions join at the corners of the (0) and (III) phases. It would also be interesting to explore more models with statistical interactions that can have such reformulations. An accessible direction already in the present setting is to examine the model Eq. (5) with general statistical angle θ . Another interesting direction is to introduce some attraction between the two loop species, to see if we can achieve fermionic bound states of J_1 and J_2 and what phases can be accessed in this way.

Acknowledgements. We are grateful to A. Vishwanath, M. P. A. Fisher, and T. Senthil for many stimulating discussions, and in particular thank A. Vishwanath for careful reading of the manuscript and useful suggestions. This research is supported by the National Science Foundation through grant DMR-0907145, and by the XSEDE computational initiative grant TG-DMR110052.

-
- ¹ A. Stern, *Annals of Physics* **323**, 204 (2008).
- ² N. Read and B. Chakraborty, *Phys. Rev. B* **40**, 7133 (1989).
- ³ A. Kitaev, *Annals of Physics* **303**, 2 (2003).
- ⁴ T. Senthil and M. P. A. Fisher, *Phys. Rev. B* **62**, 7850 (2000).
- ⁵ J. Vidal, S. Dusuel, and K. P. Schmidt, *Phys. Rev. B* **79**, 033109 (2009).
- ⁶ I. S. Tupitsyn, A. Kitaev, N. V. Prokof'ev, and P. C. E. Stamp, *Phys. Rev. B* **82**, 085114 (2010).
- ⁷ E. Fradkin and S. H. Shenker, *Phys. Rev. D* **19**, 3682 (1979).
- ⁸ T. Senthil and M. P. A. Fisher, *Phys. Rev. B* **74**, 064405 (2006).
- ⁹ C. Xu and S. Sachdev, *Phys. Rev. B* **79**, 064405 (2009).
- ¹⁰ S.-P. Kou, M. Levin, and X.-G. Wen, *Phys. Rev. B* **78**, 155134 (2008).
- ¹¹ G. Y. Cho and J. E. Moore, *Annals of Physics* **326**, 1515 (2011).
- ¹² T. Hansson, V. Oganesyan, and S. Sondhi, *Annals of Physics* **313**, 497 (2004).
- ¹³ E. Fradkin and S. Kivelson, *Nucl. Phys. B* **474**, 543 (1996).
- ¹⁴ T. Senthil, A. Vishwanath, L. Balents, S. Sachdev, and M. P. A. Fisher, *Science* **303**, 1490 (2004).
- ¹⁵ T. Senthil, L. Balents, S. Sachdev, A. Vishwanath, and M. P. A. Fisher, *Phys. Rev. B* **70**, 144407 (2004).
- ¹⁶ A. W. Sandvik, *Phys. Rev. Lett.* **98**, 227202 (2007); *Phys. Rev. Lett.* **104**, 177201 (2010).
- ¹⁷ R. G. Melko and R. K. Kaul, *Phys. Rev. Lett.* **100**, 017203 (2008).
- ¹⁸ F. Alet, G. Misguich, V. Pasquier, R. Moessner, and J. L. Jacobsen, *Phys. Rev. Lett.* **97**, 030403 (2006).
- ¹⁹ G. Chen, J. Gukelberger, S. Trebst, F. Alet, and L. Balents, *Phys. Rev. B* **80**, 045112 (2009).
- ²⁰ D. Charrier and F. Alet, *Phys. Rev. B* **82**, 014429 (2010).
- ²¹ A. Kuklov, N. Prokof'ev, and B. Svistunov, *Phys. Rev. Lett.* **92**, 030403 (2004).
- ²² A. B. Kuklov, N. V. Prokof'ev, B. V. Svistunov, and M. Troyer, *Ann. Phys. (N.Y.)* **321**, 1602 (2006).
- ²³ J. Smiseth, E. Smørgrav, E. Babaev, and A. Sudbø, *Phys. Rev. B* **71**, 214509 (2005).
- ²⁴ S. Kragset, E. Smørgrav, J. Hove, F. S. Nogueira, and A. Sudbo, *Phys. Rev. Lett.* **97**, 247201 (2006).
- ²⁵ E. V. Herland, E. Babaev, and A. Sudbø, *Phys. Rev. B* **82**, 134511 (2010).
- ²⁶ J. Lou, A. W. Sandvik, and N. Kawashima, *Phys. Rev. B* **80**, 180414 (2009).
- ²⁷ A. Banerjee, K. Damle, and F. Alet, *Phys. Rev. B* **82**, 155139 (2010); **83**, 235111 (2011).
- ²⁸ M. Kamal and G. Murthy, *Phys. Rev. Lett.* **71**, 1911 (1993).
- ²⁹ O. I. Motrunich and A. Vishwanath, *Phys. Rev. B* **70**, 075104 (2004).
- ³⁰ A. B. Kuklov, M. Matsumoto, N. V. Prokof'ev, B. V. Svistunov, and M. Troyer, *Phys. Rev. Lett.* **101**, 050405 (2008).
- ³¹ O. I. Motrunich and A. Vishwanath, eprint arXiv:cond-mat/08051494(2008).
- ³² R. Kaul and A. Sandvik, eprint arXiv:cond-mat/11104130(2011).
- ³³ M. C. Cha, M. P. A. Fisher, S. M. Girvin, M. Wallin, and A. P. Young, *Phys. Rev. B* **44**, 6883 (1991).
- ³⁴ F. Alet and E. S. Sørensen, *Phys. Rev. E* **67**, 015701 (2003).
- ³⁵ M. S. S. Challa, D. P. Landau, and K. Binder, *Phys. Rev. B* **34**, 1841 (1986).
- ³⁶ M. P. A. Fisher and D. H. Lee, *Phys. Rev. B* **39**, 2756 (1989).